

SODA: Protecting Proprietary Information in On-Device Machine Learning Models

Akanksha Atrey¹, Ritwik Sinha², Saayan Mitra², Prashant Shenoy¹

¹University of Massachusetts Amherst, ²Adobe Research

aatrey@cs.umass.edu, {risinha, smitra}@adobe.com, shenoy@cs.umass.edu

ABSTRACT

The growth of low-end hardware has led to a proliferation of machine learning-based services in edge applications. These applications gather contextual information about users and provide some services, such as personalized offers, through a machine learning (ML) model. A growing practice has been to deploy such ML models on the user's device to reduce latency, maintain user privacy, and minimize continuous reliance on a centralized source. However, deploying ML models on the user's edge device can leak proprietary information about the service provider. In this work, we investigate on-device ML models that are used to provide mobile services and demonstrate how simple attacks can leak proprietary information of the service provider. We show that different adversaries can easily exploit such models to maximize their profit and accomplish content theft. Motivated by the need to thwart such attacks, we present an end-to-end framework, *SODA*, for deploying and serving on edge devices while defending against adversarial usage. Our results demonstrate that *SODA* can detect adversarial usage with 89% accuracy in less than 50 queries with minimal impact on service performance, latency, and storage.

CCS CONCEPTS

• **Security and privacy** → **Intrusion/anomaly detection and malware mitigation**; • **Computing methodologies** → **Distributed artificial intelligence**; **Machine learning**.

KEYWORDS

on-device, machine learning, proprietary information, privacy

ACM Reference Format:

Akanksha Atrey¹, Ritwik Sinha², Saayan Mitra², Prashant Shenoy¹. 2023. SODA: Protecting Proprietary Information in On-Device Machine Learning Models. In *The Eighth ACM/IEEE Symposium on Edge Computing (SEC '23)*, December 6–9, 2023, Wilmington, DE, USA. ACM, New York, NY, USA, 12 pages. <https://doi.org/10.1145/3583740.3626617>

1 INTRODUCTION

The ubiquity of machine learning (ML) models in distributed applications such as fitness tracking, entertainment recommendations, virtual personal assistance, and social media services has changed

the way humans interact with their devices. This proliferation has led to consumers being more proactive and conscious about their choices, including about what data leaves their edge devices [11] and the need for faster response times [6]. This implies that ML-based predictions and recommendations cannot be conducted in a centralized manner and require them to be served closer to where the consumer is. For instance, consider a personalization model that takes as input the context of the user and recommends entertainment choices. With the advancement of low-end hardware technologies [1–3], this inference can be conducted on the consumer's device (i.e., mobile phone).

Conducting inference on the end user's device is advantageous in many aspects [10]. First, serving on the device reduces the service latency seen by the end user. Second, keeping the model on the device preserves user privacy as all the user data processing happens on the device. Third, on-device models are capable of running offline without continuous network connectivity to the centralized server. Lastly, running inference on the device reduces cloud compute cycles, consequently reducing costs for the service provider. However, on-device ML models are prone to exploitation since they lie outside the natural security perimeter of the service provider cloud that could detect, track, and protect against adversarial actions. We examine the privacy of on-device models from a service provider's point of view in this paper.

Previous works have proposed attacks to steal ML models in ML-as-a-service applications by training substitute models [15, 25, 29, 33]. This approach considers the model as intellectual property, necessitating considerable effort to train substitute models that exhibit comparable performance. However, once a model is deployed on the device, the primary concern shifts from model access to safeguarding the proprietary information embedded within the model. We argue that extracting proprietary information from models requires substantially fewer resources than model stealing.

In this work, we define the adversarial goal to be to steal proprietary information embedded in an ML model that is located on the device. For example, consider a bank application that produces personalized credit card offers based on users' contextual information. Assume a ML model is deployed on the edge for this purpose. Here the distribution and range of offers available along with 'who is recommended what' is proprietary information. An adversary can learn what sets of inputs give them the most profitable output by learning the probability distribution of the potential offers as shown in Figure 1a. Alternatively, consider an image authentication service that accepts or rejects images on a social media platform based on their authenticity. Here the criteria or rules embedded in the model are proprietary information. An adversary can learn the rules by investigating the model's most salient features and

Permission to make digital or hard copies of all or part of this work for personal or classroom use is granted without fee provided that copies are not made or distributed for profit or commercial advantage and that copies bear this notice and the full citation on the first page. Copyrights for components of this work owned by others than the author(s) must be honored. Abstracting with credit is permitted. To copy otherwise, or republish, to post on servers or to redistribute to lists, requires prior specific permission and/or a fee. Request permissions from permissions@acm.org.
SEC '23, December 6–9, 2023, Wilmington, DE, USA

© 2023 Copyright held by the owner/author(s). Publication rights licensed to ACM.
ACM ISBN 979-8-4007-0123-8/23/12...\$15.00
<https://doi.org/10.1145/3583740.3626617>

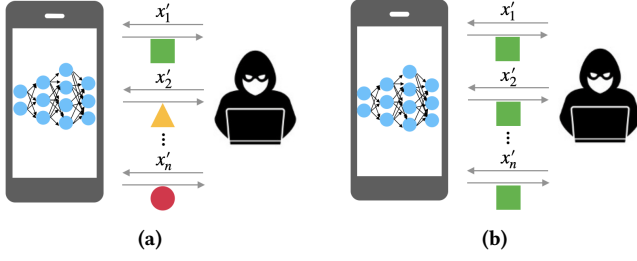


Figure 1: Examples of leaking proprietary information via on-device ML models where x'_i represents adversarial queries and shapes represent model output (e.g., service): (a) exploiting output diversity, and (b) exploiting decision boundaries of a particular service type (e.g., class).

distort the input in minor ways to authenticate disallowed images as shown in Figure 1b.

In both the examples above, a common theme is to exploit the hidden representations or input-to-output mappings that are embedded in the ML model. Often these are rules or criteria set by the service provider and are considered proprietary information. Having unauthorized access to this information is disadvantageous to the brand. Firstly, this information can be published or sold to competitors, coupon sites, or price aggregators which can affect the service provider's business. Secondly, since such systems often have a feedback loop with new streams of data being used for model updates, the adversary can poison or bias the future versions of the model with their high volume of atypical queries.

In this paper, we examine these privacy issues in on-device models from the service provider's point of view. Motivated by the need to protect the service provider's proprietary information, we propose Secure On-Device Application (*SODA*), an end-to-end system for deploying and serving on device. *SODA* defends the proprietary information in on-device ML models using an autoencoder-based approach that captures adversarial usage across time. In the design and implementation of *SODA*, we make the following contributions:

- C1 We develop a taxonomy of on-device models by examining models used in distributed services (e.g., web or mobile applications).
- C2 We demonstrate how simple privacy attacks can leak proprietary information contained in on-device models with differing levels of threats. We group these threats into white-box and black-box attacks.
- C3 We propose a robust system, *SODA*, to defend against leakage of proprietary information from on-device models. The proposed solution protects against differing levels of threats ensuring its generalizability and adaptability.
- C4 Our empirical evaluation on two widely used datasets demonstrates that *SODA* can detect adversarial usage with 89% accuracy in less than 50 queries with a minimal increase in latency.

2 BACKGROUND

In this section, we present background on distributed services and the usage of ML in such services.

2.1 Distributed Services

This work focuses on distributed services whose service components are distributed across edge devices and cloud. Traditional services host the front-end components on the edge device and back-end components on the cloud. Modern day services collect contextual data about the user and their environment to provide data-dependent services. These services can be categorized into three: one-time, occasional, and real-time. Examples of one-time services include financial offers or life insurance risk assessments. Occasional services range from health or smart home applications which are used on a per-need basis. Finally, real-time services involve mapping applications and fitness trackers. We focus on one-time and occasional services. Real-time services offer a different set of challenges due to their continuous usage.

2.2 Machine Learning in Distributed Services

Much of the data-intensive computation in distributed services is aided by data mining and ML. For example, consider ride-sharing applications which use ML for next location prediction. An ML model is typically trained on the cloud using data from many users and each service query is served through a direct call to the model's API.

With the development of low-end hardware (e.g., Apple's Neural Engine [1] and Intel's Movidius [2]), more computation is moving to the end user's device. That is, models can now be trained or fine-tuned on the edge device itself using user-specific data and can be served on the device for faster inference [8, 34]. In this work, we focus specifically on models that are deployed on edge devices for inference regardless of where they are trained. We assume the training process is kept distinct from the end user.

2.3 Privacy Attacks in Machine Learning

Data privacy has become an increasing concern with the proliferation of ML. Prior works have proposed attacks which leak information about sensitive features in the training data through model inversion [12], membership of data samples through membership inference [32], and embedded global patterns in the data through property inference [13]. Closer to our work, model extraction attacks have been proposed to leak information about the model itself to create copies of models locally [33]. This requires recursively querying the target model to build a substitute data set for training a shadow model. These types of attacks are especially harmful in ML-as-a-service applications where commercially valuable models are allowed to be used on a pay-per-query basis. While these attacks apply in on-device deployment settings, training shadow models require a sufficiently large number of queries. We instead focus specifically on the privacy of the proprietary information of the service provider embedded in ML models, which can be leaked in much fewer queries in comparison. To the best of our knowledge, no prior work considers this facet of proprietary information leakage in on-device models.

2.4 Privacy Preserving Model Serving

With the emergence of novel attacks targeting model deployment and serving, limiting queries or following black-box deployment methods are naive strategies for inference privacy. However, such

Table 1: Taxonomy of white-box (WB) and black-box (BB) ML models on the device with the components of the ML model accessible by a user.

Model Type	Feature Space		Output Space		Internals		
	All	Model Input	Model Output	Output Probabilities	Architecture	Parameters	Representations
WB	✓	✓	✓	✓	✓	✓	×
BB	✓	×	✓	×	×	×	×

methods are not always feasible, especially in distributed applications where ensuring benign users are provided appropriate service is important. More sophisticated methods have been proposed to preserve inference privacy with the goal of protecting private information in the training data. These methods rely on traditional approaches such as differential privacy, homomorphic encryption, and information theoretic privacy [22, 24, 28, 30]. However, these solutions do not consider privacy from the *service provider's standpoint* since high-level representations can still be leaked via continuous querying.

3 PRIVACY IMPLICATIONS OF ON-DEVICE MODELS

In this section, we set up the privacy problem in models that are deployed on edge devices for inference. We first present a taxonomy of on-device models and then demonstrate how such models can be attacked to leak proprietary information about the service provider.

3.1 Taxonomy of On-Device Models

An ML model can be divided into three spaces: feature space, prediction space, and internals. The feature space includes inputs to the ML system, including features that are collected by the application but not employed during the training of the model. The prediction space includes model predictions and the probabilities associated with those predictions. Finally, the internals space consists of the model architecture, parameters (e.g., weights), and hidden representations.

The deployment of ML models on the device can be categorized into white-box deployment and black-box deployment as summarized in Table 1. White-box deployment provides users transparency and access to all components in the feature and output spaces, and model parameters. This is equivalent to deploying a serialized version of the model such that it is programmatically accessible by any modern framework. Popular serialization methods include TensorFlow SavedModel, Open Neural Network Exchange (ONNX), Predictive Model Markup Language (PMML), and TorchScript. Serialized models can be deployed as an external file on a web or mobile application, and used as a library by the application. In such settings, the model is accessible via the browser's inspect element, sophisticated web scraping methods, or by accessing the application bundle¹.

Black-box deployment provides a layer of security by only revealing the inputs collected by the application and the model output. This is equivalent to deploying a model in a mobile application by embedding it into the application's binary interface. Alternatively, deploying encrypted serialized model files, adding access controls

on serialized model files, or adding secure boot and firmware protections are also black-box deployment methods. Unless the adversary has memory access, the model components are much harder to access in these situations.

3.2 Threat Model

We describe the entities of the threat model as follows.

Service Provider. We consider a service provider \mathcal{S} who is responsible for providing an arbitrary service. \mathcal{S} employs ML-based predictions to aid its service by training a general, multi-user model $M : X \rightarrow Y$ where X is contextual data and Y represents the set of possible service categories, such as credit card offers. We assume that M is a C -class model trained on the cloud, where C represents the number of distinct classes in Y (i.e., the cardinality of the response), and the training process is kept distinct from other entities in the threat model. This model is then deployed on the end user's device for serving. We assume Y and the representations learned by M are proprietary information.

User. We consider a user \mathcal{U} who uses the service provided by \mathcal{S} . We assume \mathcal{U} stores the deployed model M on their edge device and allows the service to use their contextual data, $X_{\mathcal{U}}$. \mathcal{U} is expected to accept the service (e.g., $M(X_{\mathcal{U}}) \rightarrow Y$) provided by \mathcal{S} in an honest manner.

Adversary. We consider an adversary \mathcal{A} who uses the service provided by \mathcal{S} in order to extract proprietary information about \mathcal{S} . Similar to \mathcal{U} , \mathcal{A} stores the deployed model M on their device and is expected to accept the service (e.g., $M(X_{\mathcal{A}}) \rightarrow Y$). As a baseline, the adversary has access to an organic query $x_{\mathcal{A}}$. We assume \mathcal{A} to be a curious adversary who attempts to learn $M(X'_{\mathcal{A}}) \rightarrow Y$ with two alternative goals:

- A-1** Identify all y_c where $c \in \{1, 2, \dots, C\}$ such that $M(X'_{\mathcal{A}}) \rightarrow Y$ (i.e., exploiting output diversity).
- A-2** Identify variances $x'_{\mathcal{A}} \sim x_{\mathcal{A}}$ such that $M(X'_{\mathcal{A}}) \rightarrow y_c$ (i.e., exploiting decision boundary of class c).

We explore \mathcal{A} 's ability to query the model in both white-box and black-box scenarios. Since M is stored on their device and is accessible in an offline fashion, \mathcal{A} is not bounded by query limits. We further assume the adversary lacks the capability to inspect the memory of a running program and disassemble RAM to extract executable code or the model executable.

3.3 Exploiting Proprietary Information Through Querying Attacks

While prior works have proposed attacks to steal ML models by training substitute models, the order of queries required to build a substitute model is on the scale of 1000s [15, 26, 29]. In this work,

¹Note, accessing the application bundle requires appropriate access controls.

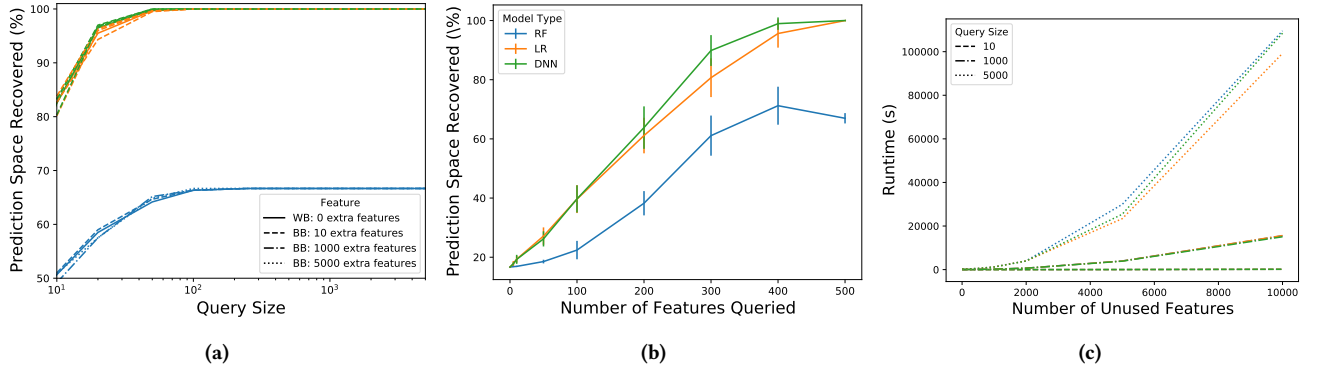


Figure 2: Results of random querying attacks on decision trees (DT), multi-class logistic regression models (LR) and deep neural networks (DNN) in white-box (WB) and black-box (BB) environments: (a) impact of query size on the classes recovered; (b) impact of the number of features queried among the model input on the classes recovered; and (c) impact of the number of unused features on runtime in the BB environment. The legend in (b) applies to all figures.

Table 2: Performance (%) of querying attacks across datasets and models. Attack A-1 demonstrates the percentage of prediction space recovered using randomly generated queries, and attack A-2 demonstrates the accuracy of exploiting decision boundaries across classes via random perturbations.

		Attack A-1	Attack A-2
HAR	Random Forest	66.33	96.18
	Logistic Regression	100.00	99.85
	Deep Neural Network	100.00	99.72
MNIST	Random Forest	29.50	98.67
	Logistic Regression	100.00	99.73
	Deep Neural Network	90.50	100.00

we demonstrate that only a limited number of queries are needed to leak proprietary information in on-device ML models. Specifically, we show querying attacks starting with a single seed query are sufficient to leak information about input-to-output mappings with as little as 50 queries. While more sophisticated methods may be used for querying, our goal is to demonstrate how simple attacks can leak varying levels of proprietary information. The simplicity of the attack is aided by the nature of on-device models which are often accessible in an offline fashion and not restricted in usage.

3.3.1 Experimental Setup. To test the efficacy of querying attacks, we use two popular datasets: (1) UCI’s human activity recognition (HAR) dataset [5], and (2) MNIST digits recognition dataset [20]. The HAR dataset consists of 561 smartphone sensor features from 30 users while performing six activities (walking, walking upstairs, walking downstairs, sitting, standing, and laying). All features are normalized and bounded to a $[-1, 1]$ scale. The training data consists of a random partition of 70% of the volunteers, while the test data comprises the remaining 30% of the participants. The MNIST dataset contains 70,000 28x28 grayscale images of handwritten digits from 0 to 9. Each pixel in the image is represented by a number from 0 to 255. We normalize the features to a $[-1, 1]$ scale and transform the images into one-dimensional vectors of 784 features. We use 60,000 images for training and the remaining 10,000 images as test data.

Table 3: Runtimes of random query attacks to recover maximum percentage of the prediction space before plateauing (A-2).

Model Type	Attack Type	Runtime (s)
RF	White-box	0.2801
	Black-box	54.2049
LR	White-box	0.0951
	Black-box	18.9895
DNN	White-box	0.0929
	Black-box	18.4184

We train random forests (RF), multi-class logistic regression models (LR) and deep neural networks (DNN) for the human activity recognition and digits recognition tasks. Optimal hyperparameters are chosen for each model by performing randomized search on 3-fold cross validation. The resulting recognition performance is 96%, 93%, and 94% for the HAR dataset respectively, and 97%, 92%, and 96% for the MNIST dataset respectively.

The attacks are conducted using 100 randomly selected organic seed queries from the test data. All results are aggregated across these 100 adversaries.

3.3.2 Exploiting Output Diversity (A-1). For adversarial goal A-1, we attempt to recover the prediction space (e.g., classes) beyond the seed query by drawing random queries from the uniform distribution. This attack can be executed by introducing randomness to either a subset or all of the features. This is equivalent to exploiting the input to receive maximally benefiting services such as highly profitable financial offers. Table 2 contains the percentage of classes recovered via 100 random queries. While random forests are more robust to the attack with only 66.33% and 29.50% attack performance on HAR and MNIST respectively, the logistic regression and neural network models leak more than 90% of the classes on both datasets.

We further examine the impact of varying attack parameters on the HAR dataset. Figure 2a demonstrates the impact of query size on the percentage of classes recovered. Despite the simplicity of

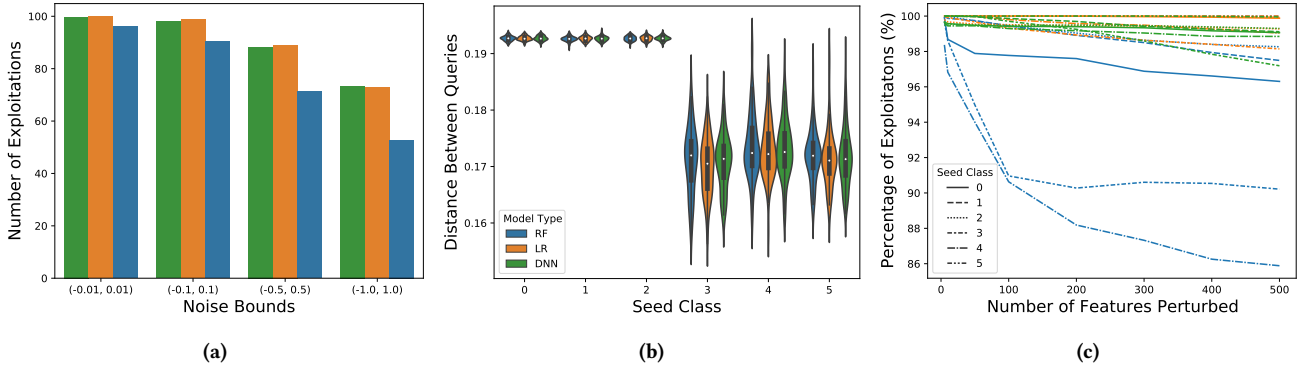


Figure 3: Results of random noise perturbation attacks to exploit decision boundaries of decision tree (DT), multi-class logistic regression model (LR) and deep neural network (DNN): (a) impact of noise bounds on the number of exploitations; (b) euclidean distance between exploitable queries for each seed class; and (c) impact of the number of features perturbed on the percentage of exploitations. The legend in (b) applies to all figures.

the attacks, we see 50%-100% leakage for different models across different number of query sizes. We also note the lower attack performance of random forests and attribute it to the robustness and unsmooth decision boundaries of ensemble modeling. Yet, we still see a $\sim 67\%$ leakage with random forests for 5000 queries.

Although there is limited distinction in leakage of white-box versus black-box models, there is a substantial difference in runtimes. Table 3 contains the runtimes of recovering the maximum percentage of prediction space before plateauing. With only 1000 extra features, the runtime of the black-box attack was up to 199 times slower. If the percentage of features used for model training is substantially lower than the total features collected, the runtime increases substantially for black-box environments. This is shown in Figure 2c where an addition of 10,000 extra features can take ~ 30 hours to run for 5000 queries. In the white-box setting, the adversary has access to the model inputs. However, with large model input sizes, the attack may be difficult.

Figure 2b demonstrates the impact of randomly selecting a subset of the features on the prediction space recovered. The random selection of the subset of features is averaged across 10 samples for 1000 queries. Even with querying only half of the features, there is up to $\sim 70\%$ leakage².

Key Takeaway: Randomly generated queries can expose up to 100% of model outputs, with random forests’ robustness attributed to their unsmooth decision boundaries. However, black-box model attacks, while equally effective, have significantly longer runtimes.

3.3.3 Exploiting Decision Boundaries (A-2). For adversarial goal A-2, we attempt to exploit the decision boundary of the seed query class. This is similar to identifying ways that the input can be perturbed while achieving the same service. Prior work in the model stealing literature has employed out-of-distribution (OOD) surrogate queries to exploit decision boundaries of the target model and train a clone model [15, 26, 29]. However, many of these sophisticated querying attacks only work for deep learning models with the

end goal of cloning the target model. We focus on exploitation of decision boundaries by maximizing the number of different queries of the same class without the need to cover any particular space.

To distort the seed input, we add random noise drawn from a uniform distribution to a subset or all the features. Table 2 contains results of adding noise drawn from $[-0.01, 0.01]$ to all the features. The results are averaged across all classes. For both datasets, small perturbations lead to a high exploitation accuracy ranging from 96.18% to 100.00%. As in the previous attack, the LR and DNN models are slightly more vulnerable than the RF model.

We further examine the impact of attack parameters on the HAR dataset. Figure 3a demonstrates the impact of noise bounds on the number of exploitations (i.e., same class queries) made. With smaller noise perturbations, exploitations are much easier to conduct as expected. Similar to the previous attack however, the random forest is more robust than the DNN and logistic regression model. With higher noise bounds, the random forest successfully exploits through only $\sim 50\%$ of the queries.

Figure 3b considers the difference in exploited queries for different seed classes with noise generated from $[-0.01, 0.01]$ bound. The required perturbations to exploit a particular class differ; while classes 0-2 require larger differences in perturbations, classes 3-5 allow more variance in perturbations leading to easability in the attack. Exploitations thus depend on the nature of the data and the impact of features on each class.

As considered in the last attack, we also consider the impact of only perturbing a subset of features. Results in Figure 3c demonstrate the lowering efficacy of the attack as more features are queried. Intuitively, this suggests that a smaller change yields the same result whereas perturbing large number of features can change the model output. This reasoning makes it much easier to conduct such an attack, both from an efficiency and latency standpoint.

Key Takeaway: Perturbation attacks on decision boundaries achieve up to 100% success with smaller bounds. While perturbing fewer features yields higher exploitation success, the impact on different classes varies.

²This may differ for different datasets depending on how important certain features are for the model.

4 PRESERVING PROPRIETARY INFORMATION IN ON-DEVICE MODELS

Deploying models on the edge device of the end user reduces the service provider's control of its usage and makes it difficult to track or identify adversarial actions. In this section, we propose an end-to-end modeling system, *SODA*, for deploying and serving ML models on user devices while protecting the proprietary information embedded in the model through an in-built defense layer.

In design of *SODA*, we account for several non-trivial challenges:

- (1) **Nature of Adversarial Queries:** As demonstrated by our simple attacks in Section 3.3, the nature of adversarial queries can vary from simple single feature perturbations to complex randomly generated queries. This randomness can lead to both in-distribution (ID) queries and out-of-distribution (OOD) queries. While prior works have considered detecting OOD queries [15, 17, 18], we make no assumptions on the distribution of the queries.
- (2) **Nature of Adversarial Goals:** As discussed in Section 3.2, adversarial goals can fall into one of two categories: (1) exploiting output diversity, and (2) exploiting decision boundaries. The nature of output expected for both these goals is opposite, requiring a complex solution that does not depend solely on output leakage for adversarial detection.
- (3) **Nature of On-Device Models:** On-device serving often supports offline access and preserves user data privacy, a major deterrence to relying on the cloud for identifying adversarial actions. The system design must thus be able to run end-to-end on the device with requiring minimal to no cloud support.

To satisfy the above challenges, *SODA*'s architecture is designed to maintain requirements of on-device models such as low latency, privacy of user data, and offline access, while defending against attacks that leak output diversity and decision boundaries of classes. The defense layer comprises of an autoencoder that is used to detect adversarial usage and label successive queries as benign or adversarial. Figure 4 demonstrates the design of *SODA*.

SODA consists of the following key components.

4.1 Autoencoder Training

The first step is to train an autoencoder to convert the input query into a lower dimensional representation. The training can occur on the cloud or edge network, unknown from the user. The autoencoder consists of an encoder f_e , which takes as input a k -dimensional query x_i and converts it into a m -dimensional vector x_e where $m < k$, and a decoder f_d , which takes as input the output of the encoder and reconstructs the original k -dimensional query x'_i .

$$\begin{aligned} f_e(x_i) : \mathbb{R}_k &\rightarrow \mathbb{R}_m \\ f_d(x_e) : \mathbb{R}_m &\rightarrow \mathbb{R}_k \end{aligned}$$

The autoencoder is trained to minimize the mean squared error loss over the training data, X_{train} as follows:

$$L(X_{\text{train}}) = \frac{1}{|X_{\text{train}}|} (X - f_d(f_e(X_{\text{train}})))^2$$

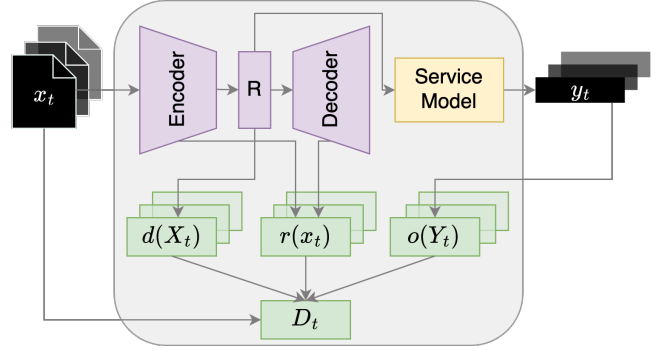


Figure 4: Overview of the proposed inference pipeline of *SODA*. The purple blocks represent the autoencoder, yellow block represents the service model, and the green blocks represent the detector mechanism where detector output D_t is an aggregation of the query distance, $d(X_t)$, reconstruction error, $r(x_t)$, and output entropy, $o(Y_t)$. Processing in the gray box occurs in memory while the application is running on the edge device and is assumed to be inaccessible by the user.

Autoencoders are a popular anomaly detection method as they fail to reconstruct anomalous inputs by design [35]. This behavior stems from training the autoencoder on a dataset comprised mostly of benign instances, thereby enabling it to accurately reconstruct such instances. When confronted with anomalous inputs, which differ significantly from the patterns learned during training, the autoencoder struggles to faithfully reconstruct them, resulting in a higher reconstruction error. The reconstruction error between the original input X_i and reconstructed input X'_i is expected to be low for ID queries and high for OOD queries. We use this aspect of autoencoders during the design of the defense layer (see Section 4.3).

4.2 Service Model Training

The second step involves training the model that is used to aid an arbitrary service (e.g., offer recommendation). As before, the training of the service model can occur on the cloud or edge network, unknown from the user. This model takes as input the output of the encoder $f_e(X_{\text{train}})$ and outputs a service Y .

$$M(f_e(X_{\text{train}})) : \mathbb{R}_m \rightarrow \mathbb{R}_c$$

The encoder maps the input data into a lower-dimensional representation, often referred to as the latent space, that captures essential features and patterns of the input data. Integrating the training of model M with an autoencoder enables M to leverage the learned latent representation and fine-tune it specifically for the targeted service, eliminating the need for relearning from raw input data. By design, the model can be of any complexity, ranging from simple linear models to more complex deep networks.

4.3 Adversarial Detection

The third step of the framework is adding the defense mechanism that guards against adversarial usage of the models described above.

SODA's defense mechanism is built upon the measurement of leakage rate (l) across time.

In order to capture the challenges with building a generalized and robust solution towards protecting proprietary information, we define leakage rate using three components. First, we capture OOD queries via the autoencoder's reconstruction error $r(x_t)$ where x_t is the k -dimensional query at time t . As discussed in Section 4.1, we exploit the fact that autoencoders are unable to reconstruct queries coming from a different distribution than the training data. We use cumulative mean squared error to calculate a moving total of the error between the original query and the reconstructed query (e.g., output of the decoder).

$$r(x_t) = r(x_{t-1}) + \frac{1}{k} \sum_{i=1}^k \left((x_t^i - f_d(f_e(x_t)))^2 \right) \quad (1)$$

The second component in the computation of leakage rate is distance between the queries $d(X_t)$ where X_t represents the set of queries $\{x_1, x_2, \dots, x_t\}$ until time t . Intuitively, we expect queries from adversaries exploiting decision boundaries to be very similar with minute perturbations whereas adversaries exploiting output diversity will have fairly different queries. By measuring the distance between the queries, we capture queries that are too similar or too different. We use the cumulative median Euclidean distance between encoded query at time t and all the previous encoded queries by the same user to identify the distance at time t . Euclidean distance is chosen as a measure of distance due to its ability to measure magnitude well.

$$d(X_t) = d(X_{t-1}) + \text{med}(\|f_e(x_i) - f_e(x_t)\| \forall i \in [0, t-1]) \quad (2)$$

The third component in the computation of leakage rate is the output entropy $o(Y_t)$ where Y_t are the set of predictions of the service model $\{y_1, y_2, \dots, y_t\}$ until time t . Entropy is a measure of the randomness or uncertainty. We use this as a measure to explore the diversity of the predictions made by the model. Intuitively, substantially high entropy would indicate diverse and varied predictions, whereas substantially low entropy would indicate similar or repetitive predictions, both of which can be suggestive towards adversarial usage. We can use the extremeness of the entropy as an indicator of adversarial usage. Let p_i represent the probability of occurrence of class c_i . Then, we have:

$$o(Y_t) = - \sum_{i=1}^C p_i \log(p_i) \quad (3)$$

All components undergo min-max normalization with respect to the training data. This normalization technique scales each component's values with respect to the minimum and maximum values observed in the training data at each time step. By applying this normalization process, the components are transformed to a standardized scale that facilitates fair and meaningful comparisons. The final computation of leakage rate l_t is an aggregation of the three components above as follows:

$$l_t = \alpha r(x_t) + \beta d(X_t) + \gamma o(Y_t) \quad (4)$$

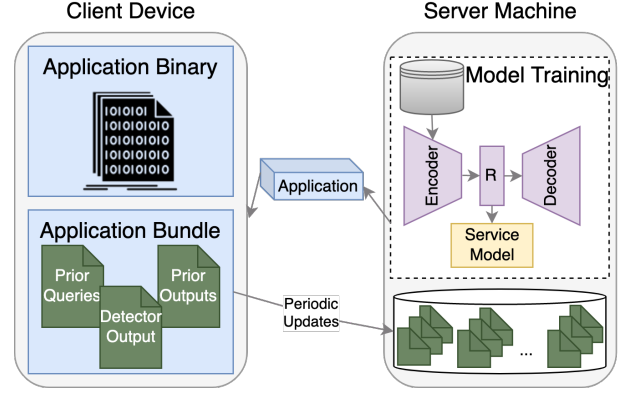


Figure 5: Overview of the model training and deployment in SODA. The application binary contains the program itself which runs in memory when the application is invoked. The application bundle contains the files the application uses, including list of encoded queries, prior model outputs and prior values of the adversarial detection layer.

where α , β and γ are the weights associated with the cumulative reconstruction error, cumulative median euclidean distance and output entropy respectively such that $\alpha + \beta + \gamma = 1$.

Finally, the detector categorizes queries observed until time t as either benign or adversarial through threshold scaling as follows:

$$D_t = \begin{cases} 1, & \text{if } l_t < l_t^{tr} - \delta l_t^{tr} \text{ or } l_t > l_t^{tr} + \delta l_t^{tr} \\ 0, & \text{otherwise} \end{cases} \quad (5)$$

Here, l_t^{tr} represents the leakage rate of the training data at time t . If the leakage rate l_t falls outside the range defined by $l_t^{tr} - \delta l_t^{tr}$ and $l_t^{tr} + \delta l_t^{tr}$, the query is classified as adversarial (1). Otherwise, it is classified as benign (0). The selection of an appropriate value for δ depends on the specific requirements and characteristics of the data. Upon detection of adversarial usage against the adversary, the system delegates the responsibility of choosing the appropriate action, such as blocking further use or implementing periodic suspension, to the service provider.

4.4 System Deployment

The fourth and final step of SODA enables secure system deployment on the device where the models are deployed in a black-box manner. Figure 5 demonstrates the design of the training and deployment process. The training steps from Sections 4.1 and 4.2 occur on the server machine (e.g., cloud). Once trained, SODA deploys the model on the user's device in a black-box manner by either embedding the model into the binary of the application or by storing the model as encrypted serialized model files. For the latter method, we use the Open Neural Network Exchange (ONNX) format to serialize model files as it is interoperable and framework-independent [4].

The model parameters (e.g., weights) and other relevant files from Section 4.3, including a list of encoded queries, prior model outputs, and prior values of the adversarial detection layer, are encrypted and stored on the device. We employ the XSalsa20 stream cipher for encryption of these files. XSalsa20 provides a high level

of security and efficiency while being well-suited for devices with limited computational power. The encryption and decryption happens in memory while the application is running and is expected to be secure from adversarial access.

Finally, *SODA* periodically uploads these data files to the cloud to ensure recovery during deletion or application reset.³ This ensures that adversaries cannot delete these files or the application and restart their attack from scratch. The frequency of the uploads along with the nature of the file monitoring can be determined by the service provider. Since the data being sent to the cloud does not contain raw queries made by the user, user data is still considered to be preserved.

5 PROTOTYPE IMPLEMENTATION

We implement a prototype of the proposed system *SODA* on a Raspberry Pi 3 (RPI) running Debian GNU/Linux 11. The RPI is equipped with a 64-bit quad-core ARM Cortex-A53 processor and 1GB RAM. The prototype is developed using Python 3.6. The remainder of this section describes our implementation of *SODA* including model training, adversarial detection, and optimizations for on-device deployment.

Model Training. *SODA* comprises of two types of models, autoencoder and service model, as described in Sections 4.1 and 4.2 respectively. The autoencoder is instantiated within the *PyTorch* framework. It consists of two `nn.Sequential()` modules, designed to serve as the encoder and decoder components. Each of these modules comprises two linear layers with a ReLU activation. Additionally, the prototype accommodates three variants of service models: random forests (RF), multi-class logistic regression (LR), and deep neural network (DNN). The DNN model, implemented using *PyTorch*, is structured with three linear layers interspersed with ReLU activations. Conversely, the RF and LR models are implemented using the *Scikit-Learn library*. The selection of optimal hyperparameters for each model is achieved through randomized search employing 3-fold cross-validation. The model training process is performed on an NVIDIA Titan-X GPU equipped with 32GB memory.

Adversarial Detection. The adversarial detection, as described in Section 4.3, involves categorizing the leakage rate via query distance, autoencoder reconstruction error, and output entropy. We leverage the *threading* library to implement multithreading, allowing for concurrent computation of the leakage rate components. Additionally, to safeguard against tampering with the output files generated during this process, we employ the *PyNaCl* library, which enables encryption through the XSalsa20 stream cipher and authentication via the Poly1305 MAC mechanism.

System Deployment. The deployment of the application inference pipeline adheres to the architectural design depicted in Figure 4. To achieve interoperability, we employ the *skl2onnx* library and the `torch.onnx.export()` function to serialize the models into the ONNX format. Furthermore, in order to further minimize the memory footprint of *PyTorch* models, dynamic quantization is employed.

³Under constraints of complete offline access, enabling user authentication and file monitoring can achieve the same goal.

Table 4: Difference between traditional serialized models and ONNX models for single query inference (aggregated across 100 queries). AE refers to the autoencoder model used in *SODA*.

	Serialization	Performance	Runtime (ms)	Size (KB)
AE	Traditional	5.75e-3	0.237	2834
	ONNX	5.86e-3	0.154	726
RF	Traditional	88.00%	13.749	4474
	ONNX	88.00%	0.250	2903
LR	Traditional	92.00%	0.217	7
	ONNX	92.00%	0.058	5
DNN	Traditional	92.00%	0.268	138
	ONNX	92.00%	0.087	37

This process converts single precision model parameters into reduced precision integer representation, without significant loss in accuracy. The efficacy of utilizing ONNX runtime in comparison to the Scikit-Learn and PyTorch frameworks is demonstrated in Table 4, showcasing substantial improvements in runtime and model size. Lastly, the inference pipeline is packaged into an executable file via the *Pyinstaller* library.

By design, when the application prototype is invoked, the detector processes the input and updates resource files in the application bundle. If the detector detects adversarial usage, the user is temporarily suspended for a designated time period. To ensure data integrity, file updates are sent to another server at frequent intervals. Finally, file monitoring is enabled such that if files in the application bundle get deleted, the application won't execute the request and the user will be blocked for a time period.

6 SYSTEM EVALUATION

In this section, we demonstrate the efficacy of employing *SODA* for on-device deployment on high-level objectives including the ability to defend against adversaries, latency, size, and performance. We employ the HAR and MNIST datasets described in Section 3.3.1 for evaluation. As before, all results are aggregated across 100 adversaries. Unless otherwise stated, the system parameters are set to $\alpha = 0.33$, $\beta = 0.33$, $\gamma = 0.33$, and $\delta = 0.2$.

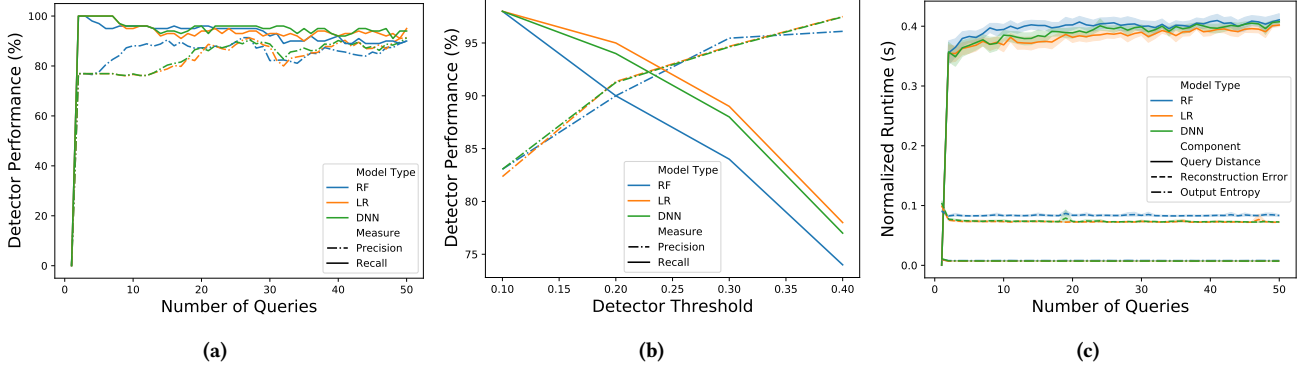
6.1 Efficacy of Adversarial Detection

To evaluate the efficacy of the adversarial detection layer, we employ the training set and test set as representative examples of benign queries. For the generation of adversarial data, we follow the methodology outlined in Section 3.3, which involves the selection of 100 random seed queries and subsequent generation of random and perturbed queries.

6.1.1 Evaluation of Detection Output. Our evaluation of the detection layer compares *SODA* with three other methods. We first compare with a random baseline which randomly labels users as benign or adversarial. The remaining two methods are chosen based on proximity to our work. Specifically, MagNet proposed a two-pronged defense against adversarial examples using an autoencoder-based approach [23]. We employ MagNet's autoencoder with an error threshold of 0.01 and 0.04 for the HAR and MNIST datasets, respectively. These thresholds were chosen

Table 5: Performance of adversarial detection in the proposed system as compared to random baseline and prior works.

Dataset	Method	Random Forest			Logistic Regression			Deep Neural Network		
		Accuracy	Precision	Recall	Accuracy	Precision	Recall	Accuracy	Precision	Recall
HAR	Random	57.69	81.69	58.00	46.92	73.85	48.00	52.31	78.79	52.00
	MagNet*	75.00	100.00	50.00	75.00	100.00	50.00	75.00	100.00	50.00
	PRADA*	77.69	77.52	100.00	77.69	77.52	100.00	78.46	78.13	100.00
	SODA	84.62	90.00	90.00	89.23	91.35	95.00	88.46	91.26	94.00
MNIST	Random	49.09	33.87	42.00	49.82	36.62	52.00	49.46	34.15	42.00
	MagNet*	75.00	100.00	50.00	75.00	100.00	50.00	75.00	100.00	50.00
	PRADA*	36.36	36.36	100.00	36.36	36.36	100.00	36.36	36.36	100.00
	SODA	94.91	100.00	86.00	92.00	100.00	78.00	93.45	100.00	82.00

**Figure 6: Results of evaluating SODA's output: (a) detector performance with respect to the number of queries (b) detector performance on 50 queries with respect to the detector threshold; and (c) runtime of the detector components with respect to the number of queries.**

based on the highest value observed in the benign set, ensuring a false positive rate of 0. We also compare with PRADA which labels successive queries as adversarial based on the distribution of distances between the queries [15]. We set the detection threshold at 0.95, signifying a greater level of confidence in the normalcy of the observed distribution. Note, these comparisons are based on re-implementations of both systems.

The detection results are compared in the form of accuracy, precision, and recall. A high precision value indicates that when the model predicts an instance as adversarial, it is likely to be correct. It is useful when the cost of false positives (misclassifying benign users as adversarial) is high. Alternatively, a high recall value indicates that the model is effective at identifying adversaries and minimizing false negatives. It is particularly important when the cost of false negatives (failing to detect adversaries) is high, as it ensures that a larger proportion of adversaries are correctly identified.

As tabulated in Table 5, SODA outperforms the other methods for 50 queries. Specifically, by combining multiple components for detection, SODA achieved $\approx 36\%$, $\approx 13\%$, and $\approx 10\%$ improvements in accuracy over the baseline, MagNet, and PRADA methods, respectively, for the HAR DNN. While precision and recall are higher for the other methods, SODA performs the most optimally on all three metrics. For instance, while MagNet has 100% precision, it fails to recognize half the adversaries as indicated by the 50% recall. Conversely, while PRADA has a 100% recall, it misclassifies many

benign users as adversarial as indicated by the 78.13% precision. This can be attributed to the different design requirements of the methods. While PRADA emphasizes long-term detection for model extraction attacks, MagNet emphasizes detection of perturbation-based adversarial attacks. SODA is a more generalizable method which incorporates different components for detecting a wider range of attacks. Similar results are noted for the random forest and logistic regression models and MNIST dataset.

Key Takeaway: The proposed system outperforms prior methods that pursued similar goals by 10%-59%. The results solidify SODA's ability to detect a wider range of attacks as shown in Section 3.3, thereby providing strong evidence about its generalizability.

6.1.2 Impact of Detection Parameters. We further evaluate resiliency of the defense mechanism across system parameters on the HAR dataset. Figure 6a demonstrates the precision and recall values of the adversarial detection layer across queries. We observe that SODA's ability to identify adversaries increases as the number of queries increases. It is important to note that precision and recall are typically inversely related. Increasing one often leads to a decrease in the other. Therefore, the choice between the two depends on the specific requirements of the system and the relative costs associated with false positives and false negatives. The effect described can be observed in Figure 6b, which showcases the influence of the detector threshold δ (as defined in Equation 5). As δ increases, the recall decreases, resulting in an increase in false negatives. In our

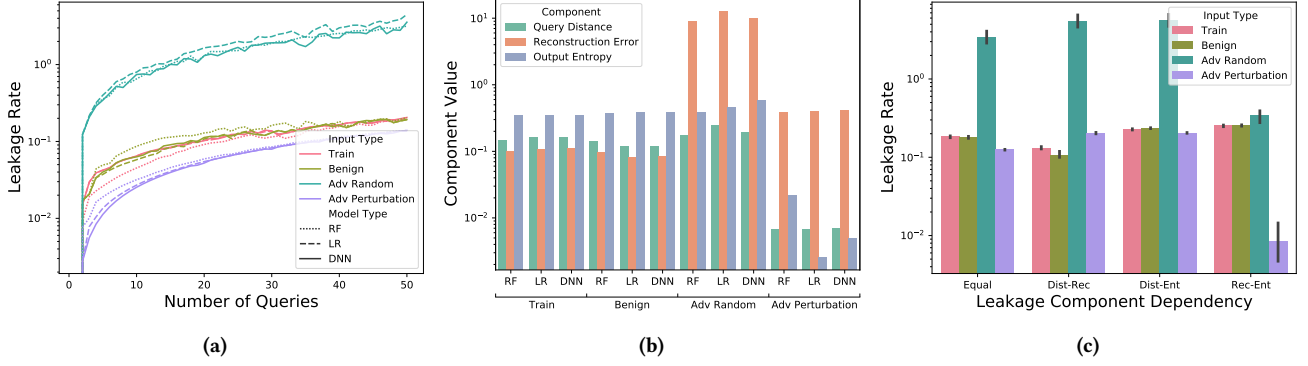


Figure 7: Results of analyzing leakage rate across input and model types: (a) leakage rate with respect to the number of queries across input and model types; (b) leakage component values across input and models types; and (c) affect of leakage component thresholds on leakage rate aggregated across models where ‘Dist’ represents distance, ‘Rec’ represents reconstruction error, and ‘Ent’ represents output entropy.

Table 6: Inference overhead of proposed system *SODA* compared to the traditional approach of on-device deployment.

Model	Method	Runtime (s)	Size (MB)	Accuracy (%)
RF	Baseline	2.086	40.51	92.50
	<i>SODA</i>	1.749	61.46	90.33
LR	Baseline	0.094	36.83	96.13
	<i>SODA</i>	0.234	58.56	92.94
DNN	Baseline	0.137	36.83	94.74
	<i>SODA</i>	0.291	58.59	92.90

use case, a threshold value of $\delta = 0.2$ strikes a balance between false positives and false negatives.

Figure 6c demonstrates the breakdown in system runtime across leakage rate components and number of queries. The computation of output entropy and reconstruction error exhibits consistent runtime, regardless of the number of queries. However, there is an increasing runtime observed for query distance computation due to the pairwise comparisons performed at each timestep. Additionally, we observe that the RF model has a higher runtime compared to the DNN and LR models, aligning with the overall longer runtime of RF inference demonstrated in Table 6.

Key Takeaway: Since *SODA* is designed around the premise of comparing consequent queries, its effectiveness in detecting adversaries grows as more queries are provided, with minimal and consistent overhead in runtime across detection components. The ability to choose the detector threshold enables further flexibility in practical deployment.

6.1.3 Analysis of Leakage Rate. To better understand the impact of leakage rate on the detection output, we perform an analysis of leakage rate across input and model types. Figure 7a showcases the impact of the number of queries on the leakage rate. While the leakage rate remains relatively consistent between the data obtained from model training and benign users across model types, a notable divergence occurs for both random and perturbed adversarial queries as the number of queries increases. This distinction corroborates the increasing recall seen in Figure 6a.

A further breakdown of the component values in the leakage rate is demonstrated in Figure 7b. As described in Section 4.3, query distance is important for identifying similarity or dissimilarity of queries over time, reconstruction error is important for identifying OOD queries, and output entropy is important for output diversity attacks. For random queries, the reconstruction error is significantly higher as compared to the error for training and benign data. Conversely, the query distance and output entropy are much lower for perturbed queries. This analysis suggests that *SODA* effectively handles the differing nature of adversarial queries by leveraging different components in the leakage rate.

Lastly, we examine the influence of parameters in Equation 4. Visible differences are observed for random and perturbed queries when equal dependency is assigned to the parameters (e.g., $\alpha = 0.33$, $\beta = 0.33$, $\gamma = 0.33$). Conversely, focusing on reconstruction error and output entropy only (e.g., $\alpha = 0.5$, $\beta = 0$, $\gamma = 0.5$) suggests a larger distinction for perturbed queries and a smaller distinction for random queries. While the choice of parameter dependency can be tailored based on the system requirements, it is important to note that all three components of the leakage rate contribute value to the adversarial detection process.

Key Takeaway: The analysis of leakage rate reinforces the effectiveness of *SODA* by revealing distinct detection patterns across benign and adversarial usage. While each component of the leakage rate contributes value to the detection of adversaries, it is possible to assign dependency to these components based on the application requirements.

6.2 Overhead of Proposed System

We also examine the overhead of inference with *SODA* with the goal that *SODA* should not exert significant additional overhead compared to the baseline method of using the service model directly. The results are shown in Table 6 for the HAR dataset.

While there is a minor loss in accuracy across service model types, the inclusion of an autoencoder and adversarial detection layer in the inference pipeline leads to an approximate 50% increase in the overall application size. However, a significant increase in

Table 7: Summary of existing defenses against model extraction attacks comparing edge friendliness, model interoperability, and adaptability across adversaries.

Type	Method	Edge-Friendly	Interoperable	Adaptable
Protection	Protecting parameters with differential privacy [33]	×	✓	✓
	Training with adversarial diversity [17, 29]	×	✓	×
	Modifying prediction probabilities [21, 27, 33]	✓	✓	×
	Adaptively misinforming for OOD queries [18]	✓	×	×
Detection	Quantifying feature space explored [19]	✓	×	✓
	Evaluating closeness to decision boundaries [31]	✓	✓	×
	Analyzing query distribution [14, 15, 23]	✓	✓	×
	Analyzing queries and output leakage (SODA)	✓	✓	✓

storage comes from the *scipy* library used for computation of leakage rate components. With additional mathematical optimizations in the implementation, the dependency on this library can be removed, reducing the application size further.

We also note the ~ 1.4 -fold and ~ 1.1 -fold times increase in inference runtime for the LR and DNN models respectively. However, it is important to note that the tradeoff between runtime and protection of proprietary information may not negatively impact the user experience given the generally low inference times (< 0.3 seconds). Conversely, there is a ~ 0.16 -fold decrease in query runtime for the RF model. We hypothesize this is due to the RF’s sensitivity towards the number of input features; since the autoencoder converts the input into a lower dimensional vector, the RF has to compute fewer operations, resulting in improved runtime efficiency. For all model types, the adversarial detector ran concurrently with the inference service, averaging to 0.158 seconds.

Key Takeaway: While prioritizing higher service provider privacy adversely affects storage, runtime, and accuracy, this tradeoff can be deemed insignificant in practice. By enabling the detector to run in the background for the previous timestep, the service latency is unaffected by the detector.

7 RELATED WORK

Model extraction attacks aim to learn information about the model itself. They use a trained ML model to extract model parameters and learn an equivalent shadow model to poison with adversarial examples [25, 29] or monetize off of the model in ML as a service applications [33]. Since training data is often unavailable, extraction attacks employ querying techniques to exploit the model. Beyond random querying methods, more sophisticated methods have been used where datasets from similar domains have been considered [9, 26] or synthetic queries have been objectively crafted [15, 16, 29]. However, most applications of model extraction have been motivated by user privacy. That is, the privacy issue has revolved around learning sensitive information from the training data. Closer to our work, prior works have examined model extraction attacks in security applications such as spam or fraud detection [7]. Here the goal was to evade detection using the extracted model. We explore a more generic approach for on-device deployment.

Towards preventing such attacks, prior works have proposed methods to detect and prevent adversarial usage. We present these in Table 7. Papernot et al. employed two existing methods in adversarial ML, namely adversarial training and defensive distillation for DNNs [29]. Tramer et al. discussed rounding confidence scores and

using differential privacy on training points or model parameters as potential defense mechanisms [33]. Kariyappa et al. proposed training an ensemble of diverse models with a diversity objective that requires models in the ensemble to produce dissimilar predictions [17]. However, these protection methods are not fully generalizable across model types, primarily being applicable to DNN-based models only.

Juuti et al. proposed the first generic technique to detect model extraction attacks using analysis of successive queries by checking for deviations from normal distribution [15]. However, they assume on-device deployment relies on platform security mechanisms to provide localized isolation preventing white-box attacks. Furthermore, their detection process starts when a client queries at least 100 samples. Our work proposes an end-to-end solution that effectively thwarts extraction attacks in both white-box and black-box scenarios. Furthermore, our approach promptly identifies adversarial behavior from the initiation of usage, ensuring early detection and prevention.

Other works have proposed perturbing OOD queries with adaptive misinformation [18] or modifying prediction probabilities [27, 33]. However, these works assume adversarial queries are OOD in nature. Furthermore, modifying predictions based on usage may not be applicable in situations where maintaining application performance for benign users is a critical requirement.

8 CONCLUSION

In this work, we examined the implication of leaking proprietary information in ML models deployed on user devices through querying attacks. Our results demonstrated that such attacks can be used to recover up to 100% of the output space and exploit decision boundaries with a 100% success rate. We proposed an end-to-end framework, *SODA*, that supports the deployment of ML-based applications on user devices. In *SODA*, we introduced an adversarial detection layer that leverages an autoencoder model to classify usage type as benign or adversarial. Our evaluation of *SODA*, conducted on two widely-used datasets, demonstrates its ability to detect adversarial usage with an 89% accuracy within a small number of queries.

Although *SODA* has exhibited effectiveness against simpler attacks targeting on-device models, we acknowledge the need for future research to explore more intricate attack scenarios. Additionally, examining the effect of colluding adversaries and expanding the attacks to generative AI models, which are inherently different

from classification models examined in this paper, are interesting scopes for future work.

ACKNOWLEDGMENTS

We thank the anonymous reviewers for their helpful comments. We also thank Meet Vadera, Priyanka Mammen, Bhawana Chhagani, and Phuthipong Bovornkeeratiroj for their feedback. This research was supported in part by NSF grants 2211302, 2211888, 2213636, 2105494, 1908536, Army Research Lab contract W911NF-17-2-0196 and Adobe. Any opinions, findings, and conclusions, or recommendations expressed in this material are those of the authors and do not necessarily reflect the views of the funding agencies.

REFERENCES

- [1] 2017. Apple's 'Neural Engine' Infuses the iPhone With AI Smarts. www.wired.com/story/apples-neural-engine-infuses-the-iphone-with-ai-smarts/.
- [2] 2019. Intel Vision Accelerator Design With Intel Movidius Vision Processing Unit (VPU). <https://software.intel.com/en-us/iot/hardware/vision-accelerator-movidius-vpu#specifications>.
- [3] 2019. The NVIDIA EGX Platform for Edge Computing. <https://www.nvidia.com/en-us/data-center/products/egx-edge-computing/>.
- [4] 2019. Open Neural Network Exchange. <https://onnx.ai/>. Accessed on 01/18/2022.
- [5] Davide Anguita, Alessandro Ghio, Luca Oneto, Xavier Parra, Jorge Luis Reyes-Ortiz, et al. 2013. A public domain dataset for human activity recognition using smartphones.. In *Esann*.
- [6] Ioannis Arapakis, Xiao Bai, and B Barla Cambazoglu. 2014. Impact of response latency on user behavior in web search. In *Proceedings of the 37th international ACM SIGIR conference on Research & development in information retrieval*.
- [7] Giuseppe Ateniese, Luigi V Mancini, Angelo Spognardi, Antonio Villani, Domenico Vitali, and Giovanni Felici. 2015. Hacking smart machines with smarter ones: How to extract meaningful data from machine learning classifiers. *International Journal of Security and Networks* (2015).
- [8] Akanksha Atrey, Prashant Shenoy, and David Jensen. 2021. Preserving Privacy in Personalized Models for Distributed Mobile Services. *IEEE International Conference on Distributed Computing Systems* (2021).
- [9] Jacson Rodrigues Correia-Silva, Rodrigo F Berriel, Claudine Badue, Alberto F de Souza, and Thiago Oliveira-Santos. 2018. Copycat cnn: Stealing knowledge by persuading confession with random non-labeled data. In *International Joint Conference on Neural Networks (IJCNN)*. IEEE.
- [10] Google Developers. 2022. Why On-Device Machine Learning? <https://developers.google.com/learn/topics/on-device-ml/learn-more>.
- [11] Susen Döbelt, Markus Jung, Marc Busch, and Manfred Tscheligi. 2015. Consumers' privacy concerns and implications for a privacy preserving Smart Grid architecture—Results of an Austrian study. *Energy Research & Social Science* (2015).
- [12] Matt Fredrikson, Somesh Jha, and Thomas Ristenpart. 2015. Model inversion attacks that exploit confidence information and basic countermeasures. In *ACM SIGSAC Conference on Computer and Communications Security*.
- [13] Karan Ganju, Qi Wang, Wei Yang, Carl A Gunter, and Nikita Borisov. 2018. Property inference attacks on fully connected neural networks using permutation invariant representations. In *Proceedings of the ACM SIGSAC Conference on CCS*.
- [14] Kathrin Grosse, Praveen Manoharan, Nicolas Papernot, Michael Backes, and Patrick McDaniel. 2017. On the (statistical) detection of adversarial examples. *arXiv preprint arXiv:1702.06280* (2017).
- [15] Mika Juuti, Sebastian Szyller, Samuel Marchal, and N Asokan. 2019. PRADA: Protecting Against DNN Model Stealing Attacks. In *IEEE European Symposium on Security and Privacy (EuroS&P)*. IEEE.
- [16] Sanjay Kariyappa, Atul Prakash, and Moinuddin K Qureshi. 2021. Maze: Data-free model stealing attack using zeroth-order gradient estimation. In *Proceedings of the IEEE/CVF Conference on Computer Vision and Pattern Recognition*.
- [17] Sanjay Kariyappa, Atul Prakash, and Moinuddin K Qureshi. 2021. Protecting dnns from theft using an ensemble of diverse models. In *International Conference on Learning Representations*.
- [18] Sanjay Kariyappa and Moinuddin K Qureshi. 2020. Defending against model stealing attacks with adaptive misinformation. In *Proceedings of the IEEE/CVF Conference on Computer Vision and Pattern Recognition*.
- [19] Manish Kesarwani, Bhaskar Mukhoty, Vijay Arya, and Sameep Mehta. 2018. Model extraction warning in MLaaS paradigm. In *Proceedings of the 34th Annual Computer Security Applications Conference*.
- [20] Yann LeCun and Corinna Cortes. 2010. The MNIST Database of Handwritten Digits. <http://yann.lecun.com/exdb/mnist/>.
- [21] Taesung Lee, Benjamin Edwards, Ian Molloy, and Dong Su. 2019. Defending against neural network model stealing attacks using deceptive perturbations. In *IEEE Security and Privacy Workshops (SPW)*. IEEE.
- [22] Jian Liu, Mika Juuti, Yao Lu, and Nadarajah Asokan. 2017. Oblivious neural network predictions via minionn transformations. In *Proceedings of the ACM SIGSAC Conference on Computer and Communications Security*.
- [23] Dongyu Meng and Hao Chen. 2017. Magnet: a two-pronged defense against adversarial examples. In *Proceedings of the ACM SIGSAC conference on computer and communications security*.
- [24] Fatemehsadat Mireshtghallah, Mohammadkazem Taram, Prakash Ramrakhiani, Ali Jalali, Dean Tullsen, and Hadi Esmaeilzadeh. 2020. Shredder: Learning noise distributions to protect inference privacy. In *Proceedings of the International Conference on Architectural Support for Programming Languages and Operating Systems*.
- [25] Seong Joon Oh, Bernt Schiele, and Mario Fritz. 2018. Towards reverse-engineering black-box neural networks. In *Proceedings of the International Conference on Learning Representations*.
- [26] Tribhuvanesh Orekondy, Bernt Schiele, and Mario Fritz. 2019. Knockoff nets: Stealing functionality of black-box models. In *Proceedings of the IEEE/CVF conference on computer vision and pattern recognition*.
- [27] Tribhuvanesh Orekondy, Bernt Schiele, and Mario Fritz. 2019. Prediction poisoning: Towards defenses against DNN model stealing attacks. *arXiv preprint arXiv:1906.10908* (2019).
- [28] Nicolas Papernot, Martín Abadi, Ulfar Erlingsson, Ian Goodfellow, and Kunal Talwar. 2017. Semi-supervised knowledge transfer for deep learning from private training data. *Proceedings of the International Conference on Learning Representations* (2017).
- [29] Nicolas Papernot, Patrick McDaniel, Ian Goodfellow, Somesh Jha, Z Berkay Celik, and Ananthram Swami. 2017. Practical black-box attacks against machine learning. In *Proceedings of the ACM on Asia Conference on CCS*.
- [30] Nicolas Papernot, Patrick McDaniel, Xi Wu, Somesh Jha, and Ananthram Swami. 2016. Distillation as a defense to adversarial perturbations against deep neural networks. In *IEEE Symposium on Security and Privacy (S&P)*. IEEE.
- [31] Erwin Quiring, Daniel Arp, and Konrad Rieck. 2018. Forgotten siblings: Unifying attacks on machine learning and digital watermarking. In *IEEE European symposium on security and privacy (EuroS&P)*. IEEE.
- [32] Reza Shokri, Marco Stronati, Congzheng Song, and Vitaly Shmatikov. 2017. Membership inference attacks against machine learning models. In *IEEE Symposium on Security and Privacy*.
- [33] Florian Tramèr, Fan Zhang, Ari Juels, Michael K Reiter, and Thomas Ristenpart. 2016. Stealing machine learning models via prediction apis. In *Proceedings of the USENIX Security Symposium*.
- [34] Seunghyun Yoon, Hyeonju Yun, Yuna Kim, Gyu-tae Park, and Kyomin Jung. 2017. Efficient transfer learning schemes for personalized language modeling using recurrent neural network. *AAAI Workshop on Crowdsourcing, Deep Learning, and Artificial Intelligence Agents* (2017).
- [35] Chong Zhou and Randy C Paffenroth. 2017. Anomaly detection with robust deep autoencoders. In *Proceedings of the ACM SIGKDD International Conference on Knowledge Discovery and Data Mining*.